Proceedings of the Canadian Society for Mechanical Engineering International Congress 2022
CSME Congress 2022
June 5-8, 2022, Edmonton, AB, Canada

NUMERICAL MODELING OF GRAVITY DECANTATION TANK FOR MINE-WATER TREATMENT IN UNDERGROUND MINES

Mahmoud A. Alzoubi*, Antoine Monot, Philippe-Olivier Provost, David Rancourt, Sébastien Poncet
Department of Mechanical Engineering, Université de Sherbrooke, Sherbrooke, QC, Canada
*email: mahmoud.alzoubi@usherbrooke.ca

Abstract— Reducing the overall mine-water consumption is a necessity in moving toward a more sustainable mining industry in Canada. Water treatment is a key requirement to achieve this goal. This study numerically investigates the dynamics of a decantation process as a technique to recycle and reuse mine-water. A three-dimensional mathematical model that considers the conservation of mass and momentum has been derived, validated, and implemented to simulate the turbulent two-phase flow inside a decantation tank. The framework of the validated model has been extended to examine the effect of various design and operating parameters on the efficiency of a full-scale decantation tank. The results compare the efficiency of multiple designs of the decantation tank in terms of the overflow water quality. The results indicate that the efficiency of the decantation tank increases with inner surface area, where a plain decanter with a tangential inlet pipe has the highest efficiency.

Keywords: decantation; water treatment; underground mine; two-phase flow; numerical modeling

I Introduction

Mine-water consumption in underground mines has increased dramatically in recent years due to the escalating demand for metals and minerals and the decrease in the overall ore quality [1]. According to Environment and Climate Change Canada, the mining sector consumed more than 975 million cubic meters of water in 2013, with a 25% increase from 2011 [2]. 73% of the mine-water is used as process water that serves various purposes such as drilling, slurry transport, dust suppression, mineral processing, and others. Recycling process water is an essential step to reduce the total intake of raw water while at the same time minimizing the release of potentially contaminated mine-water to the surrounding environment. Modern mines often recycle most of the process water [3]. However, there are various technical obstacles to reusing mine-water, including water quality and quantity, and treatment cost and complexity [4].

There are several treatment approaches to recycle process water. The selection and configuration of these approaches depend mainly on site conditions such as process water quantity, available space, and chemical compositions of the mined minerals [5]. For instance, remote deep mines often treat their process water underground. The key benefits from implementing this local approach are reducing the pumping cost and its corresponding impacts, such as lowering energy load, maintenance cost, biological activity, and the dependence on the chemical supply chain [6].

One of the local methods to treat mine-water is the coagulation–flocculation–decantation process. This effective physical–chemical pre-treatment technique has been widely used in industrial wastewater treatment [7–9], dye effluents [10], and others to force the suspended solids to agglomerate into large settleable flocs in order to improve water recovery from concentrate. The decantation sub-process is classically designed to separate and trap suspended solids based on the differences in their densities. The implementation of the decantation process in the mining industry goes way back to 1905 when the Dorr thickener was invented and introduced in the mining concentrators of South Dakota [11]. Since then, the technique has been utilized alone or in combination with other processes to recycle and reuse process water [12, 13].

Several studies have discussed the process of a batched thickener tank [14–17]. However, the research of a continuous decantation process is scarce, especially for underground mining applications. Therefore, the goal of this paper is to characterize the dynamics of the separation process within a gravity decantation tank under various design and operating conditions. A three-dimensional model is derived and implemented in this research to mimic the corresponding physics of the decantation of solid particles.

In the following, the model derivation along with its numerical implementation are discussed in Section II. The results are then discussed and explained in Section III. Here, we analyze the outcomes of a parametric study that highlights the impact of the design and operating parameters of a decantation tank. Finally, we draw various conclusions remarks on our research, emphasizing the effect of the inlet flow rate, tank internal design, and the orientation of the inlet pipe on the overall efficiency of the decantation tank.

II Model Development

A Geometrical modeling

Fig. 1 shows a schematic diagram of a decantation tank with a tangential inlet pipe and an inner cylinder. The latter serves as an obstacle that aims to reduce the inlet velocity. The decanter has an overall diameter of 1003.3 [mm] (39.5 [in]). The diameter of the inner cylinder

Support from NSERC, Technosub, and HPC facilities of Compute Canada

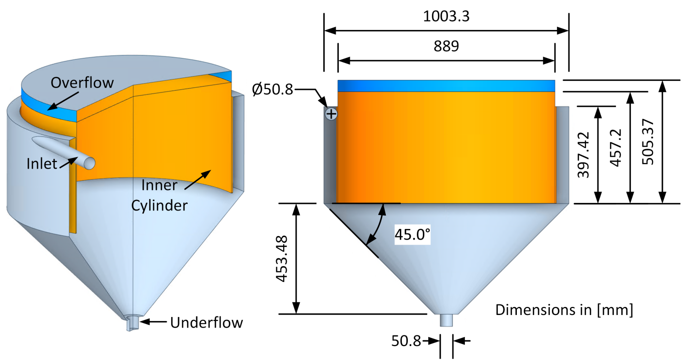

Figure 1. Schematic diagram of a full-scale decantation tank with an inner cylinder.

is 889 [mm] (35 [in]) which leaves a gap of 57.15 [mm] (2.25 [in]) between the outer wall of the decanter and the inner cylinder. This gap is slightly bigger than the 50.8 [mm] (2 [in]) diameter of the inlet pipe, which forces the inlet flow to slide over the wall of the inner cylinder aiming to reduce the tangential inlet velocity. The decanter is divided into two main sections with a total height of 958.85 [mm] (37.75 [in]), excluding the underflow pipe. The first part is the vertical top cylinder with a height of 505.37 [mm]. This section consists of the inner cylinder with a height of 457.2 [mm] (18 [in]), the inlet pipe, and the overflow with a height of 48.17 [mm]. The clean water exits the decantation tank through the overflow into a bucket (not shown in the schematic). It is then collected to be either reused or go through further recycling processes. The second part is a 45° cone with a height of 453.48 [mm]. The aim of the angled cone is to ease the settlement and the collection of the flocculants through the underflow pipe. The design shown in Fig. 1 is used as a base-case design in this study. We compare the impact of various design concepts on the overflow water quality; more elaboration on this point is given in the following sections.

B Governing Equations

A three-dimensional mathematical model comprising the conservation equations of mass and momentum is derived to govern the isothermal, two-phase, steady-state, turbulent flow of water and solid flocculated particles inside the decantation tank. The turbulent flow model is formulated based on the Reynolds-Averaged Navier-Stokes equations using the ε-based Reynolds Stress Model (RSM) based on Launder, Reece, and Rodi model [18]. The Eulerian-Eulerian approach is employed to model the two-phase flow by describing the liquid-particle and particle-particle interactions. The two-phase flow is characterized by the concept of phasic volume fractions,φ, as a continuous spatial function:

— Conservation of mass:

$$\nabla\cdot(\varphi_\ell\rho_\ell\mathbf{u}_\ell)=0 \qquad (1)$$

$$\nabla\cdot(\varphi_s\rho_s\mathbf{u}_s)=0 \qquad (2)$$

where ρ is the density and $\mathbf{u}$ is the velocity vector for liquid phase, ℓ, and solid phase, s.

— Conservation of momentum:

$$\nabla\cdot(\varphi_\ell\rho_\ell\mathbf{u}_\ell\otimes\mathbf{u}_\ell)=-\varphi_\ell\nabla p\mathbf{I}+\nabla\cdot\tau_\ell+\varphi_\ell\rho_\ell\mathbf{g}+\mathbf{F}_{\mathrm{lift},\ell}+\mathbf{F}_{R_{\ell s}} \qquad (3)$$

$$\nabla\cdot(\varphi_s\rho_s\mathbf{u}_s\otimes\mathbf{u}_s)=-\varphi_s\nabla p\mathbf{I}+\nabla\cdot\tau_s+\varphi_s\rho_s\mathbf{g}+\mathbf{F}_{\mathrm{lift},s}+\mathbf{F}_{R_{s\ell}} \qquad (4)$$

where p is the pressure shared by all phases, $\mathbf{I}$ is the identity index, τ is the stress-strain tensor, $\mathbf{g}$ is the gravitational acceleration, $\mathbf{F}_{\mathrm{lift}}$ is the lift force, and $\mathbf{F}_{R_{\ell s}}$ and $\mathbf{F}_{R_{s\ell}}$ are the interaction forces between the liquid and solid phases.

The liquid phase stress-strain tensor, τ_ℓ, is defined as below:

$$\tau_\ell=\varphi_\ell\mu_\ell\left(\nabla\mathbf{u}_\ell+(\nabla\mathbf{u}_\ell)^T-\frac{2}{3}(\nabla\cdot\mathbf{u}_\ell)\mathbf{I}\right)+\varphi_\ell\xi_\ell\nabla\cdot\mathbf{u}_\ell\mathbf{I} \qquad (5)$$

where μ and ξ are the shear and bulk viscosities, respectively. On the contrary, the solid phase stress-strain tensor, τ_s is defined based on the kinetic theory of granular flow with the addition of solid pressure p_s term into the equation [19]:

$$\tau_s=-p_s\mathbf{I}+\varphi_s\mu_s\left(\nabla\mathbf{u}_s+(\nabla\mathbf{u}_s)^T-\frac{2}{3}(\nabla\cdot\mathbf{u}_s)\mathbf{I}\right)+\varphi_s\xi_s\nabla\cdot\mathbf{u}_s\mathbf{I} \qquad (6)$$

The lift force, $\mathbf{F}_{\mathrm{lift},\ell}$ and $\mathbf{F}_{\mathrm{lift},s}$, are defined as below [20]:

$$\mathbf{F}_{\mathrm{lift},\ell}=-C_l\rho_\ell\varphi_s(\mathbf{u}_\ell-\mathbf{u}_s)\times(\nabla\times\mathbf{u}_\ell) \qquad (7)$$

$$\mathbf{F}_{\mathrm{lift},s}=-C_l\rho_s\varphi_\ell(\mathbf{u}_s-\mathbf{u}_\ell)\times(\nabla\times\mathbf{u}_s) \qquad (8)$$

where C_l is the lift coefficient that is defined based on Moraga's model [20].

The interaction force F_R between the liquid phase and solid phase is simply defined based on the momentum exchange coefficients, $\mathbf{K}_{\ell s}(=\mathbf{K}_{s\ell})$, as [19]:

$$\mathbf{F}_{R_{\ell s}}=\mathbf{K}_{\ell s}(\mathbf{u}_\ell-\mathbf{u}_s) \qquad (9)$$

and

$$\mathbf{F}_{R_{s\ell}}=\mathbf{K}_{s\ell}(\mathbf{u}_s-\mathbf{u}_\ell) \qquad (10)$$

The momentum exchange coefficients, $\mathbf{K}_{\ell s}$ and $\mathbf{K}_{s\ell}$, are defined in this study based on the Gidaspow drag model [21].

C Numerical Methodology

Various computational domains based on multiple inlet pipe orientations and internal design of a decantation tank are developed and meshed with proper boundary conditions. The governing equations together with boundary conditions are solved using a finite-volume solver. An inhomogeneous two-phase Eulerian-Eulerian is used with an implicit volume fraction parameter that is more suitable for a steady-state simulation. The primary phase is water, while the secondary phase is modeled as a flocculed particles with a density of 1150 [m^3/s] and a diameter of 150 [μm]. These data are extracted from experiments (not shown here for sake of brevity) on the real sludge. The equations are solved with a second-order upwind spatial discretization and implementing the Semi-Implicit Pressure-Linked Equation (SIMPLE) algorithm. The convergence criteria are set to 10^{-3} for all parameters. The framework of the numerical model was carefully validated in our previous work [22] against two experimental data of turbulent pipe flow of slurries [23], and a hydrocyclone [24]. The validation results showed that the numerical model's framework was in very good agreement with the experimental data.

D Boundary Conditions

The boundary condition at the inlet is defined as a constant velocity inlet corresponding to a volumetric flow rate of 11.356 [m^3/hr] (50 [GPM]); these values are chosen based on the industry partner specific needs. It corresponds to a constant inlet velocity of 1.5564 [m/s] imposed for both phases. The turbulence is defined at the inlet based on the intensity and hydraulic diameter. The value of the turbulence intensity is set at 5%. A flocculant concentration of 4.5 % volume fraction is also defined at the inlet. A zero gauge pressure is defined at the overflow and the underflow along with zero normal gradients of each phase mass fraction. A no-slip boundary condition and a zero species flux are designated at the walls. The top of the tank, however, is defined as a slip-wall with zero shear condition to model the open-top of the decantation tank.

III Results and Discussion

This study aims at quantifying the performance of a decantation tank, in terms of the overflow water quality, under various design and operating conditions. First, a parametric study based on the decantation tank from our previous work [22] is conducted to examine various operating conditions, as depicted in Fig. 2. We examine the impact of flocs diameter, flocs inlet volume fraction, and inlet flow rate on the performance of the decantation tank. A range of flocs diameters of 10, 50, 80, 100, 150, and 200 [μm] is determined in the simulations. The inlet volume fractions range between 0.5% and 2% with an increment of 0.5%. Flow rates of 2.27, 4.54, 6.81, 9.08, and 11.36 [m^3/hr] (10, 20, 30, 40, and 50 [GPM]) are considered here. After that, a base case from the first parametric study is adopted to examine various design parameters such as inlet pipe orientation as well as various inner obstacles.

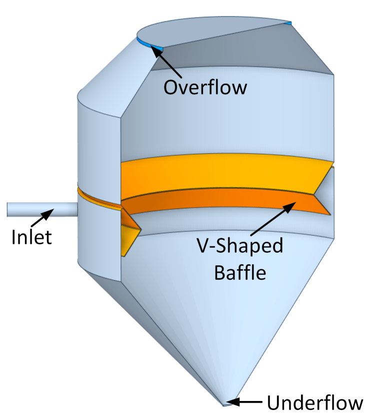

Figure 2. Schematic diagram of the decantation tank with an inner V-shaped baffle, after [22].

A Effect of Flocs Diameter

The impact of the flocs diameter on the overflow water quality is illustrated in Fig. 3. In this study, the overflow water quality is determined based on the relative volume fraction, ζ, defined as the ratio between the overflow volume fraction, φ_{out}, and the inlet volume fraction, φ_{in}, of solid particles:

$$\zeta = \frac{\varphi_{out}}{\varphi_{in}} \tag{11}$$

The relative volume fraction decreases from 88.8% at flocs diameter of 10 [μm] to as low as zero percent at flocs diameter of 200 [μm]. Additionally, flocs diameters less than 150 [μm] have a higher probability of more than 65% to appear in the overflow.

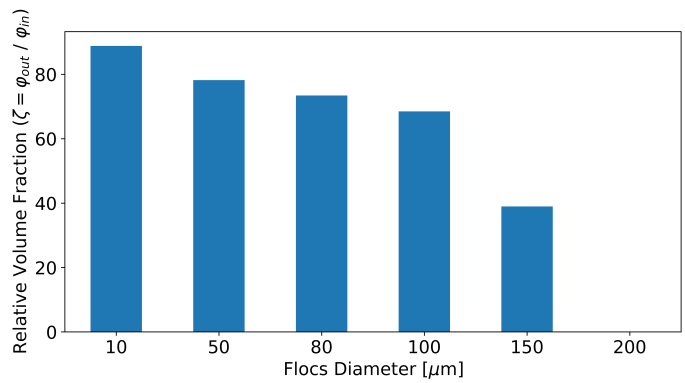

Figure 3. Influence of the flocs diameter on the overflow water quality given in terms of relative volume fraction (the lower, the better).

The flocs diameter has a linear correlation with the lift coefficient, C_l; more details are given in [19, 22]. As the diameter increases, the lift coefficient increases, which means that more force is needed to lift the flocs, as explained in Eq. (8). Therefore, as the flocs diameter increases, the probability of those flocs reaching the top of the decantation tank decreases, resulting in a lower relative volume fraction, ζ. Among other diameters, the flocs diameter of 150 [μm] exhibits the most interesting results with a relative volume fraction of 39%. This means that almost half of the flocs exit the tank through the overflow while the rest either accumulate at the bottom or exit through the underflow pipe. We chose the 150[μm] diameter as a pre-determined operating condition in the second parametric study because of its sensitive behaviour.

B Effect of Inlet Volume Fraction

Fig. 4 shows the impact of inlet volume fraction, φ_{in}, of a flocs diameter of 10 [μm] on the overflow water quality in terms of the overflow volume fraction, φ_{out}. The selection of the 10 [μm] diameter is based on the fact that it has the highest relative volume fraction, ζ, of 88.8%, as compared to the other flocs diameters, as explained in Fig. 3. Moreover, the overflow water quality is represented here in terms of overflow volume fraction, φ_{out}, instead of the relative volume fraction, ζ, because the flocs diameter is fixed. Thus, the relative volume fraction remains always the same (i.e., 88.8%). For example, in the case of an inlet volume fraction of 1.5%, the overflow volume fraction is 1.332%, which gives us a relative volume fraction of 88.8%.

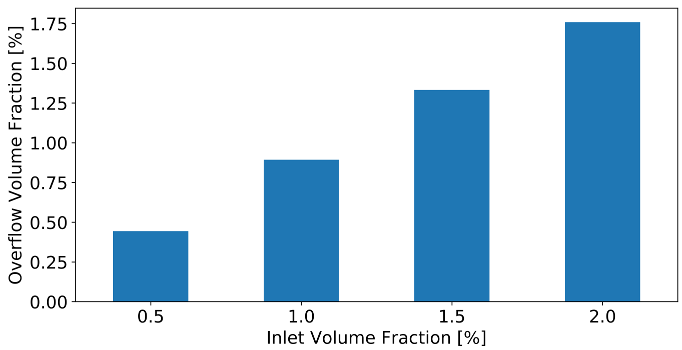

Figure 4. Influence of the inlet volume fraction, φ_{in}, on the overflow volume fraction, φ_{out}, for 10 [μm] diameter flocs.

Since the relative volume fraction is bonded with the diameter and the correlation between the lift coefficient, C_l, and the diameter is linear, as explained before, one could expect a linear correlation between the inlet and outlet volume fractions. Therefore, this linear behaviour could be extended as long as other parameters are kept constant. The inlet volume fraction of 4.5% is determined for the design parametric study based on in situ data from an underground mine.

C Effect of Inlet Flow Rate

The inlet flow rate is one of the most important parameters that affect the efficiency of the decantation process. A range of flow rates between 2.27 and 11.36 [m^3/hr] (10 and 50 [GPM]) is investigated with an increment of 2.27 [m^3/hr] (10 [GPM]) to mimic the inlet flow rate in practice. The impact of the inlet flow rate on the relative volume fraction is illustrated in Fig. 5. Here, a flocs diameter of 150 [μm] and an inlet volume fraction of 4.5% are implemented based on the previous discussion. The results show an increase in the relative volume fraction, ζ, from 0.55% at an inlet flow rate of 2.27 [m^3/hr] (10 [GPM]) to 42.3% at an inlet flow rate of 11.36 [m^3/hr] (50 [GPM]). This increase appears to be almost linear throughout the range.

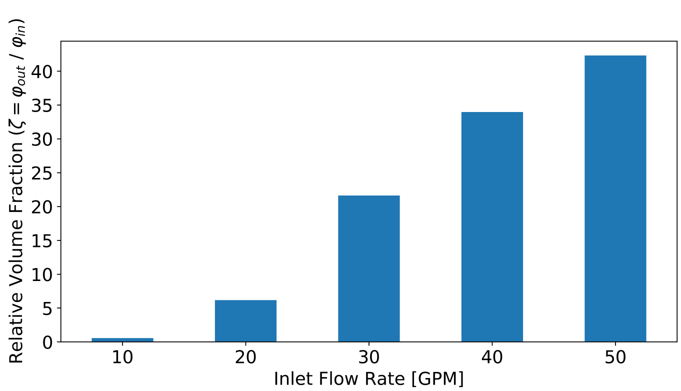

Figure 5. Influence of the inlet flow rate on the overflow water quality.

By increasing the inlet flow rate, the amount of solid particles entering the decantation tank increases, which satisfies Eqs. (1) and (2). In the light of the previous discussion on the impact of the inlet volume fraction on the overflow volume fraction, and since there are more solid particles at higher flow rates, it is expected to have a higher relative volume fraction at a higher inlet volume fraction.

D Effect of Various Design Parameters

Based on previous discussion, the operating conditions are fixed to a flocs diameter of 150 [μm], an inlet volume fraction of 4.5%, and an inlet volume flow rate of 11.36 [m^3/hr] (50 [GPM]). The second parametric study examines two main design criteria: the orientation of the inlet pipe, and the inner obstacles that aim at slowing down the flow velocity in order to improve the decantation process. The inlet pipe has either tangential or perpendicular orientations, as depicted in Fig. 6. In both cases, the pipe is installed horizontally at the top of the inner cylinder. For the plain decanter, the pipe is moved toward the bottom of the top part with a vertical tilt of 20°, aiming to increase the residence time inside the tank by directing the flow downward toward the cone. The inner cylinder and the cross structure are installed as obstacles that serve two main objectives: (i) slow down the velocity of the inlet flow, and (ii) help the solid particles decant at the bottom of the tank and then exit through the underflow pipe. These objectives should serve the ultimate goal of improving the efficiency of the decantation tank by increasing the overflow water quality. The dimensions of the inner cylinder have been discussed in Section II.A. On the other hand, the cross structure height is set at 304.8 [mm] (12 [in]); two-third of the inner cylinder height. The other dimensions such as the tank total diameter and height, the diameter of the inner pipe, the overflow height, cone angle, and diameter of the underflow pipe are kept the same, as illustrated in Fig. 1.

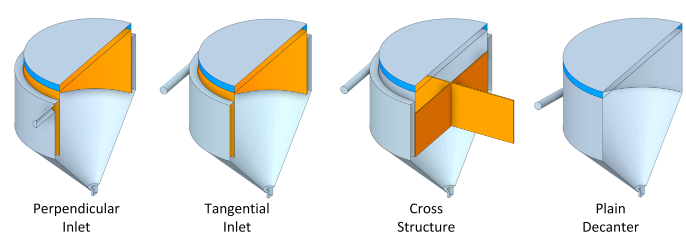

Figure 6. Various design proposals of the decantation tank.

The relative volume fraction, ζ, of each design concept is illustrated in Fig. 7, where the lower value of ζ means a better overflow water quality. First, the perpendicular inlet pipe provides the highest relative volume fraction compared to the other cases, with a value of 52%. Although the inlet flow hits the inner cylinder perpendicularly, which should result in a sudden decrease in the inlet velocity, yet more than 50% of the inlet solid particles manage to reach the overflow. This is directly correlated to the high inlet flow rate of 11.36 [m^3/hr] (50 [GPM]). The high inlet flow forces the mixture to split around the inner cylinder and form two counter swirls that negatively impact the decantation process, as depicted in Fig. 8(a). Here, a slice of a vertical plane illustrates the impact of the inlet pipe orientation at high inlet flow rate on the flocs distribution, and thus the overflow water quality.

The second observation is that the plain decanter (i.e., no obstacles) provides the lowest relative volume fraction with a value of 20.88%. Although this result sounds counterintuitive, there is a reasonable explanation behind it. The inlet flow rate enters the decantation tank through a 20° inclined tangential pipe, as shown in Fig. 6. The tangential flow creates a swirl inside the decantation tank, where heavy solid particles stay at the sidewall due to the cyclone effect. This behaviour helps the flocs decant faster into the bottom of the tank. Besides, the surface area of a plain decanter is larger than the other design concepts. A vertical plain showing the volume fraction of the solid particles is illustrated in Fig. 8(d). Since the flow rate is constant, the larger surface area leads to a lower vertical velocity. Based on the definition of lift force, $\mathbf{F}_{lift,s}$, in Eq. (8) the lower the velocity, the lower the lift force, which also leads to a lower relative volume fraction at the overflow. These two reasons explain why the plain decanter provides the lowest ζ value compared to the other design concepts.

Finally, The two main obstacles, the inner cylinder and the cross structure, perform as expected, with a relative volume fraction of 42.3% and 37.14%, respectively. However, the cross structure exhibits better performance because of the considerable disturbance to the mixture flow, leading to a lower velocity and a lower relative volume fraction. However, as shown in Fig. 8(b) & (c), there is a fundamental difference between the two designs. The decanter equipped with only an inner cylinder behaves similarly to the plain decanter, where the tangential inlet flow creates a swirl forcing the heavy solid particles to stay at the sidewall. This behaviour leads to a low value of ζ at the overflow. On the contrary, the swirl is absent in the decanter equipped with the cross structure. Instead, the cross structure halts the swirl, significantly reducing the flow velocity and ζ at the overflow.

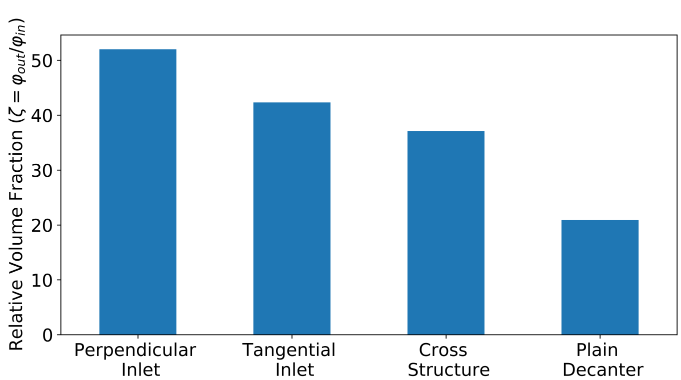

Figure 7. Overflow water quality in terms of relative volume fraction for four designs.

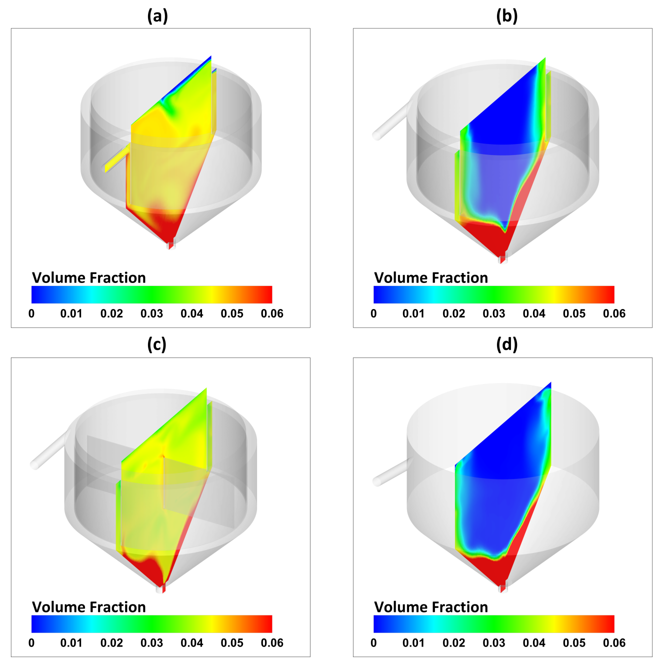

Figure 8. Contours of the flocs volume fraction for various design proposals: (a) Perpendicular Inlet, (b) Tangential Inlet, (c) Cross Structure, and (d) Plain Decanter.

Conclusions

A three-dimensional mathematical model based on the Eulerian-Eulerian approach and the RSM has been derived and implemented to model a two-phase, steady-state, turbulent flow of water and 150 [μm] flocculated solid particles. A Two-step parametric study that aims to evaluate the impact of various operating and design parameters has been conducted. First, the effect of flocculated particles diameter, inlet volume fraction, and inlet volume flow rate on the overflow water quality is studied. After that, a base case based on the first parametric study is selected as pre-determined operating conditions for the second parametric study, where various design concepts are evaluated. The results show that the surface area of a decantation tank is a crucial parameter in the efficiency of the decantation process. Moreover, certain obstacles have the ability to slow down the flow velocity, which enhances the overflow water quality. This study is a foundation for future investigations. The computational research presented here can be extended to examine a more realistic floc diameter distribution. Additionally, other design concepts could be proposed to improve the decantation process while keeping the flow rate as high as possible.

References

[1] Calvo, G., Mudd, G., Valero, A., and Valero, A., 2016. "Decreasing ore grades in global metallic mining: A theoretical issue or a global reality?". *Resources,* ***5***(36).

[2] Environment and Climate Change Canada, 2016. Canadian Environmental Sustainability Indicators: Water Withdrawal and Consumption by Sector.

[3] Gunson, A., Klein, B., Veiga, M., and Dunbar, S., 2012. "Reducing mine water requirements". *Journal of Cleaner Production,* ***21***(1), pp. 71–82.

[4] Miller, K. D., Bentley, M. J., Ryan, J. N., Linden, K. G., Larison, C., Kienzle, B. A., Katz, L. E., Wilson, A. M., Cox, J. T., Kurup, P., Van Allsburg, K. M., McCall, J., Macknick, J. E., Talmadge, M. S., Miara, A., Sitterley, K. A., Evans, A., Thirumaran, K., Malhotra, M., Gonzalez, S. G., Stokes-Draut, J. R., and Chellam, S., 2021. "Mine water use, treatment, and reuse in the United States: A look at current industry practices and select case studies". *ACS ES&T Engineering,* ***in press***.

[5] Northey, S. A., Mudd, G. M., Werner, T. T., Haque, N., and Yellishetty, M., 2019. "Sustainable water management and improved corporate reporting in mining". *Water Resources and Industry,* ***21***(100104).

[6] Gunson, A. J., 2013. "Quantifying, reducing and improving mine water use". PhD thesis, University of British Columbia.

[7] Ayeche, R., 2012. "Treatment by coagulation-flocculation of dairy wastewater with the residual lime of National Algerian Industrial Gases Company (NIGC-Annaba)". *Energy Procedia,* ***18***, pp. 147–156.

[8] Verma, A. K., Dash, R. R., and Bhunia, P., 2012. "A review on chemical coagulation/flocculation technologies for removal of colour from textile wastewaters". *Journal of Environmental Management,* ***93***(1), pp. 154–168.

[9] Azimi, S. C., Shirini, F., and Pendashteh, A., 2021. "Treatment of wood industry wastewater by combined coagulation–flocculation–decantation and fenton process". *Water Environment Research,* ***93***(3), pp. 433–444.

[10] Allegre, C., Maisseu, M., Charbit, F., and Moulin, P., 2004. "Coagulation–flocculation–decantation of dye house effluents: Concentrated effluents". *Journal of Hazardous Materials,* ***116***(1-2), pp. 57–64.

[11] Concha, F., and Bürger, R., 2003. "Thickening in the 20th century: A historical perspective". *Mining, Metallurgy & Exploration,* ***20***(2), pp. 57–67.

[12] Bosman, D., 1974. "The improved densification of sludge from neutralized acid mine drainage". *Journal of the Southern African Institute of Mining and Metallurgy,* ***74***(9), pp. 340–348.

[13] Concha, F., and Bürger, R., 2002. "A century of research in sedimentation and thickening". *KONA Powder and Particle Journal,* ***20***, pp. 38–70.

[14] Günthert, F., 1984. "Thickening zone and sludge removal in circular final settling tanks". *Water Science and Technology,* ***16***(10-11), pp. 303–316.

[15] Rudman, M., Paterson, D., and Simic, K., 2010. "Efficiency of raking in gravity thickeners". *International Journal of Mineral Processing,* ***95***(1-4), pp. 30–39.

[16] White, R., Sutalo, I., and Nguyen, T., 2003. "Fluid flow in thickener feedwell models". *Minerals Engineering,* ***16***(2), pp. 145–150.

[17] Gheshlaghi, M. E., Goharrizi, A. S., and Shahrivar, A. A., 2013. "Simulation of a semi-industrial pilot plant thickener using CFD approach". *International Journal of Mining Science and Technology,* ***23***(1), pp. 63–68.

[18] Launder, B. E., Reece, G. J., and Rodi, W., 1975. "Progress in the development of a Reynolds-stress turbulence closure". *Journal of Fluid Mechanics,* ***68***(3), pp. 537–566.

[19] Wang, X., Cui, B., Wei, D., Song, Z., He, Y., and Bayly, A. E., 2021. "CFD simulation of tailings slurry thickening in a gravity thickener". *Powder Technology,* ***392***, pp. 639–649.

[20] Moraga, F., Bonetto, F., and Lahey, R., 1999. "Lateral forces on spheres in turbulent uniform shear flow". *International Journal of Multiphase Flow,* ***25***(6-7), pp. 1321–1372.

[21] Gidaspow, D., Bezburuah, R., and Ding, J., 1991. Hydrodynamics of circulating fluidized beds: Kinetic theory approach. Tech. rep., Illinois Institute of Technology.

[22] Monot, A., Sekrani, G., Rancourt, D., and Poncet, S., 2021. "Numerical modeling of a wastewater settling tank for deep mines using an eulerian-based model". In 15th International Conference on Heat Transfer, Fluid Mechanics and Thermodynamics (HEFAT), pp. 1592–1597.

[23] Kaushal, D., Sato, K., Toyota, T., Funatsu, K., and Tomita, Y., 2005. "Effect of particle size distribution on pressure drop and concentration profile in pipeline flow of highly concentrated slurry". *International Journal of Multiphase Flow,* ***31***(7), pp. 809–823.

[24] Delgadillo, J. A., and Rajamani, R. K., 2007. "Exploration of hydrocyclone designs using computational fluid dynamics". *International Journal of Mineral Processing,* ***84***(1-4), pp. 252–261.